

Correlations and confinement in non-planar two-dimensional dimer models

Anders W. Sandvik

Department of Physics, Boston University, 590 Commonwealth Avenue, Boston, Massachusetts 02215

R. Moessner

Laboratoire de Physique Théorique de l'Ecole Normale Supérieure, CNRS-UMR8549, Paris, France

(Dated: July 12, 2005)

We study classical hard-core dimer models on the square lattice with links extending beyond nearest-neighbors. Numerically, using a directed-loop Monte Carlo algorithm, we find that, in the presence of longer dimers preserving the bipartite graph structure, algebraic correlations persist. While the confinement exponent for monomers drifts, the leading decay of dimer correlations remains $1/r^2$, although the logarithmic peaks present in the dimer structure factor of the nearest-neighbour model vanish. By contrast, an arbitrarily small fraction of next-nearest-neighbor dimers leads to the onset of exponential dimer correlations and deconfinement. We discuss these results in the framework of effective theories, and provide an approximate but accurate analytical expression for the dimer correlations.

PACS numbers: 74.20.Mn, 75.10.-w, 05.10.Ln, 05.50.+q

I. INTRODUCTION

Dimer models have a venerable history in statistical physics.^{1,2,3,4} More recently, they have also emerged as central models in modern theories of strongly correlated quantum systems, e.g., high-temperature superconductors and frustrated antiferromagnets.^{5,6,7,8,9,10,11,12,13,14} There, dimers can represent singlet-forming electron pairs. In order to model the quantum fluctuations of the dimers and realize a short-range version of Anderson's resonating valence bond (RVB) state,^{15,16} Kivelson, Rokhsar, and Sethna introduced a Hamiltonian with a resonance term which flips pairs of parallel dimers on the two-dimensional (2D) square lattice.⁵ The purely classical dimer model also retains its relevance here; it was shown that the equal-weight sum over all dimer configurations is a ground state of the Hamiltonian when the resonance strength equals the potential energy cost of each resonating pair of dimers (the RK point).⁶ The equal-time dimer correlations of the quantum dimer model are thus those of the classical dimers,¹⁷ and the imaginary time dynamics can be related to a classical random walk in configuration space.^{18,19,20}

The dimer pair correlations of the classical square lattice model decay with distance as r^{-2} and two inserted test monomers are correlated with each other as $r^{-1/2}$.⁴ As it turned out, away from the RK point the dimers form long-range order and the monomers are exponentially confined.^{7,21,22} Hence this system does not give rise to the desired RVB state with no broken lattice symmetries and deconfined monomers (corresponding to spin-charge separation¹⁶). More recently, it was shown that a true extended RVB phase *does* appear in the quantum dimer model on the triangular lattice.⁹ Following this insight, further work has been carried out in order to characterize classical and quantum dimer models on various lattices. Moreover, there are currently intense activities in gauge theories related to quantum dimer models.^{8,12,14,23,24}

To date, research on dimer models in two dimensions has focused mainly on planar lattices, i.e., ones that have no intersecting links. This class of models can be analytically solved, using Fermionic path integrals, with the aid of a theorem by Kastelyn.³ Thus the quantum ground states at the corresponding RK points are characterized as well. This body of analytical work has established a number of properties of classical dimer models which are believed to hold true even for non-planar lattices. The basis for this belief is provided by effective theories incorporating those exact results. Such effective theories are expected to be more robust than the exact solubility, and therefore not crucially dependent on lattice planarity. Consequently, there have been relatively few numerical studies testing these beliefs,²⁵ although it is not necessarily the case that the range of behaviours unearthed so far in fact exhausts all possibilities. In this paper, we provide a detailed study addressing some of these issues. We do this by considering two extensions of the square lattice dimer model which preserve its full symmetry.

The first case we consider here is a nonbipartite model with nearest-neighbour (N_1) and next-nearest-neighbour (N_2) dimers. Such bonds will inevitably appear in realistic systems away from the limiting cases represented by the nearest-neighbor (N_1) dimer models. Introducing next-nearest-neighbor links along only one of the diagonals destroys the square lattice symmetry and instead yields the topology of the triangular one. It has already been shown that an arbitrarily small fraction of such diagonal dimers destroys the critical N_1 square-lattice state and leads to deconfinement,^{14,26,27} as in the isotropic triangular lattice.⁹ The model with links along both diagonal directions, i.e., the full 2D square lattice with N_1 and N_2 bonds, is not solvable by Kastelyn's theorem.³ One would suspect (see e.g. Ref. 28) that the critical state is immediately destroyed in this case as well but this has not been explicitly demonstrated. Similarly, one might speculate that introducing longer bonds between the two

sublattices does not lead to deconfinement, but there are no exact results to back this up. For this reason, we also study the bipartite lattice with N_1 and fourth-nearest-neighbors (N_4 , of which there are eight per site).

In both the above cases, we use an efficient directed-loop^{29,30} Monte Carlo algorithm to sample the full space of hard-core dimer configurations, with fugacities w_i assigned to the different dimer types N_i . We then discuss our results in the framework of effective and simple microscopic analytic treatments. We confirm that a low (most likely infinitesimal)³² concentration of N_2 dimers leads to deconfinement; in particular, we find that the finite correlation lengths for monomers and dimers induced by the presence of the N_2 dimers scales inversely to their fugacity; $\xi \propto 1/w_2$. By contrast the presence of N_4 dimers preserves the algebraic decay of dimer correlations, $\sim 1/r^2$. These correlations have a complex dipolar structure in reciprocal space, which implies that they do not lead to a logarithmic divergence of the structure factor for $w_4 \neq 0$; such a divergence is present for the pure N_1 model. For these observations, we provide an approximate analytical theory based on the height model in the Coloumb gas representation and a self-consistent mean field solution of a large- N generalization of the dimer model.

Our numerical simulations show that the confinement exponent governing the monomer correlation function drifts, changing continuously from $-1/2$ in the pure N_1 case to $-1/9$ (to high numerical accuracy) for the pure N_4 model. In the language of height models, this corresponds to a decrease of the stiffness induced by the addition of longer-ranged dimers. Note that for the pure N_4 model, like for the soluble dimer and six-vertex models, the stiffness appears to be a simple rational number. The efficient directed loop algorithm provides an efficient direct determination of this quantity in general.

The outline of the remainder of the paper is the following: In Sec. II we introduce the directed-loop algorithm for a wide class of dimer models, and in in Sec. III we present simulation results. In Sec. IV we qualitatively explain the numerical findings based on the height-model/Coulomb-gas representation of bipartite dimer models and their large- N generalizations. We conclude in Sec. V with a summary and a brief discussion of the relevance of our study to RVB physics.

II. DIRECTED-LOOP ALGORITHM

This algorithm is an adaptation of a quantum Monte Carlo method,^{29,30} with the same name, in which updates of the system degrees of freedom are carried out along a self-intersecting path at the endpoints of which there are defects not allowed in the configuration space contributing to the partition function. When the two defects meet they annihilate, the loop closes, and a new allowed configuration is created. The conditions for detailed balance in the process of stochastically moving one of the defects are

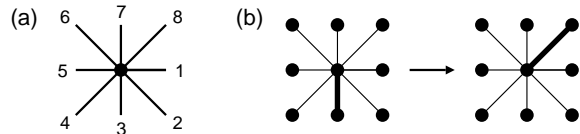


FIG. 1: (a) Labeling of the links of the N_1 - N_2 dimer model. (b) A step in the directed-loop update, in which the entrance to the vertex is at site 3 and the exit is at site 8. The thick bond indicates the location of the dimer.

expressed as a coupled set of *directed-loop equations*,²⁹ The applicability of this scheme to dimer models was first realized by Adams and Chandrasekharan.³¹ Here an algorithm for the multi-length dimer problem will be presented; a simplifying representation of the dimer configurations will also be introduced. The algorithm will be described only for the case of the N_1 - N_2 model, but the scheme applies directly to any range of the links.

The links connected to a given site are labeled as shown in Fig. 1(a). For a dimer configuration on a periodic $L \times L$ lattice, each site is numbered according to the type of dimer it is connected to. For any given site, the other member of the same dimer can then be easily found. The central object in the directed-loop algorithm is a *vertex*, which in this case consists of a site and all its surrounding sites to which it can be coupled by a dimer. The state of the vertex is the number (1-8) assigned to the central site. A step in the directed-loop algorithm is illustrated in Fig. 1(b). The vertex is entered through the dimer, and one of the seven other surrounding sites is chosen as the exit. The dimer is then flipped from the entrance to the exit, the central vertex site remaining connected to it. The exit site already has another dimer connected to it, and this site now becomes the entrance in the next step of the algorithm. In each step a defect is hence moved one link ahead, leaving behind a healed dimer state. The first entrance site is chosen at random and the corresponding defect remains stationary. It is annihilated when the moving defect reaches it, whence a new allowed dimer configuration has been generated. In the present case the defects are monomers, and the intermediate two-monomer configurations can thus be used to determine the correlations between two inserted test monomers.

The key to an efficient algorithm of this kind is that the probabilities for random selection of the seven possible exit sites can be chosen in such a way that detailed balance is satisfied without any further accept/reject criterion. Each step then moves one dimer, and a full loop can accomplish very significant changes to the dimer configuration. The directed-loop equations²⁹ give the conditions for detailed balance in terms of weights a_{jk} for the processes in which a vertex in state j is entered at site j and exited at k (transforming the vertex into state k). The actual probabilities $P_{jk} = a_{jk}/w_j$, which implies $\sum_k a_{jk} = w_j$. Detailed balance is satisfied if $a_{jk} = a_{kj}$. In the N_1 - N_2 model, the vertices can be classified as even (e) or odd (o) according to the numbering of Fig. 1(a);

there are then four weights: $a_{ee}, a_{oo}, a_{eo}, a_{oe}$. In principle, one can include “bounce” processes where $j = k$, but in the present case they can be excluded. Including only the seven no-bounce exits, the directed-loop equations reduce to

$$w_1 = 3a_{oo} + 4a_{oe}, \quad (1a)$$

$$w_2 = 3a_{ee} + 4a_{eo}, \quad (1b)$$

$$a_{eo} = a_{oe}. \quad (1c)$$

This system is underdetermined and has an infinite number of postive-definite solutions. Here the following solution will be used: For $w_1 \geq w_2$,

$$a_{ee} = a_{oe} = a_{eo} = w_2/7, \quad (2a)$$

$$a_{oo} = (w_1 - 4w_2/7)/3, \quad (2b)$$

while for $w_2 \geq w_1$,

$$a_{oo} = a_{oe} = a_{eo} = w_1/7, \quad (3a)$$

$$a_{ee} = (w_2 - 4w_1/7)/3. \quad (3b)$$

There is no guarantee that this is the best solution, but the resulting algorithm performs very well and allowed for studies of lattices with $\sim 10^6$ dimers. The fugacity of the N_1 -bonds is set to unity (except in the case of the pure N_2 - and N_4 -models). The program was tested using known results for the pure N_1 case⁴ and by comparing with local Metropolis simulations for small lattices.

III. SIMULATION RESULTS

Dimer-dimer correlations in the full close-packed system and monomer-monomer correlations in the system with two test monomers will be discussed. The monomer correlations $M(\mathbf{r})$ were obtained by accumulating the distances between the stationary and the moving monomer in the directed-loop update. As has become customary, the normalization $M(r=1) = 1$. Several types of dimer-dimer correlations can be defined. Here $D_\Sigma(\mathbf{r})$ will be defined in the following way: If site i is connected to a dimer in the set Σ , a variable $s(i) = 1$, otherwise $s(i) = 0$. The correlation function $D_\Sigma(\mathbf{r}_{ij})$ is then given by the connected correlator $\langle s(i)s(j) \rangle$. Results will be presented for cases where Σ contains a single dimer or half of the dimers of a given type (i.e., two neighboring N_1 or N_2 dimers or four neighboring N_4 dimers connected to a site i). For the N_1 - N_2 model, the correlation functions D_1 , D_2 , D_A , and D_B are thus defined corresponding to the sets $\{1\}$, $\{2\}$, $A = \{1, 3\}$, and $B = \{2, 4\}$. Analogous definitions are used for correlations D_1 , D_A of N_1 dimers and D_4 , D_D of N_4 dimers in the N_1 - N_4 model.

A. Deconfinement in the N_1 - N_2 model

In Fig. 2(a), dimer correlations D_A for the nonbipartite N_1 - N_2 model with $w_2 = e^{-4}$ (corresponding to a concentration $p_2 \approx 0.3\%$ of N_2 dimers) are compared with

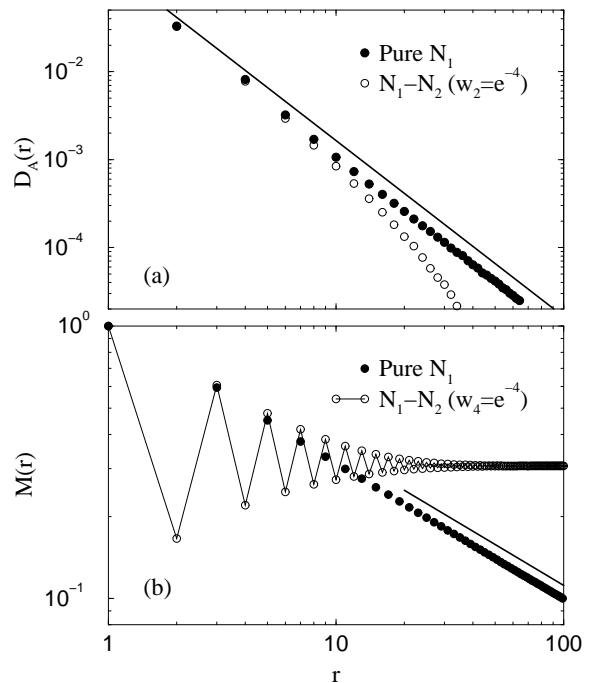


FIG. 2: Dimer (a) and monomer (b) correlations along the direction $(r, 0)$ for the N_1 - N_2 model at $w_2 = e^{-4}$, compared with those of the pure N_1 model. The solid lines show the agreement with the known power-law⁴ for the N_1 model. Note that for the pure N_1 model $M(r) = 0$ for even r . The results were obtained using $L = 1024$ lattices.

those of the pure N_1 model. There is a clear deviation from the r^{-2} decay, showing that the behaviour of the N_1 - N_2 model is fundamentally different even at this very low concentration of N_2 dimers. As shown in Fig. 2(b), the test monomer correlation approaches a nonzero constant, i.e., the system is deconfined in contrast to the algebraically confined N_1 model. The very significant changes seen already at a very low concentration of N_2 dimers suggest that an arbitrarily small concentration indeed causes deconfinement.

How does deconfinement set in upon inclusion of N_2 dimers? To address this question, we have simulated the N_1 - N_2 model for different (small) values of w_2 ranging from $e^{-3} \approx 1.5\%$ to $e^{-6} \approx 0.0086\%$. We analyze the correlation functions using a data collapse with a scaling function of the form $r^{-\alpha}\Phi(r/\xi)$. With $\xi \sim 1/w_2$ and α the respective exponent for the correlations at $w_2 = 0$, we obtain a reasonable data collapse, as shown in Fig. 3. The data for monomers is easier to handle as the algebraic decay is less rapid. We have also tried to improve the data collapse by adjusting the exponent α . We find the best-fit values $\alpha = 2.0 \pm 0.1$ and 0.55 ± 0.05 for the dimers and monomers, respectively, consistent with them remaining at their RK point values in this regime.

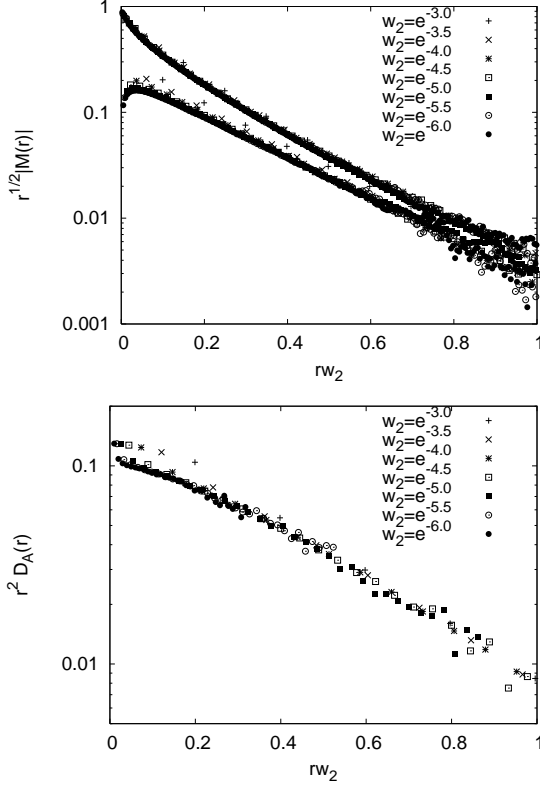


FIG. 3: Scaling collapse of monomer (top panels) and dimer (bottom panels) correlations as the fugacity w_2 is varied. The two distinct sets of points in the upper panel correspond to even and odd distances.

B. Correlations in the N_1 - N_4 model

Turning now to the bipartite N_1 - N_4 model, its dimer correlations $D_A(r)$ (involving N_1 dimers) and $D_D(r)$ (involving N_4 dimers) are compared with $D_A(r)$ of the pure N_1 model in Fig. 4. Both correlation functions appear asymptotically to decay according to the same form r^{-2} as $D_A(r)$ of the pure N_1 model. Interestingly, although $D_D(r)$ is much smaller in magnitude than $D_A(r)$ at small w_4 , it reaches the asymptotic form at shorter distances. In Fig. 5 the Fourier transforms of the correlation functions D_1 and D_4 (involving a single dimer) are shown for the pure N_1 and N_4 models. For the N_1 model, the dominant correlations are at $\mathbf{q} = (\pi, 0)$. Using finite-size scaling, a logarithmic divergence of the peak height with the system size can easily be observed (not shown here). As this feature masks some non-diverging correlations on the contour plot, we have cut it off to display more clearly, most notably, a non-analytic bow-tie feature at (π, π) .

In the N_4 model, the logarithmic peak is absent, and the correlations display a rather more complex structure, exhibiting very broad peaks, and again a bow-tie visible at the zone corner; this is rotated with respect to the bow-tie for N_1 dimers. These features show almost no

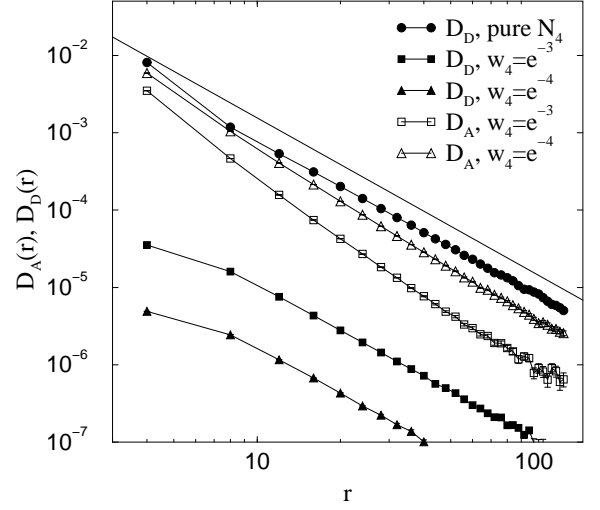


FIG. 4: Various dimer correlations along the direction $(r, 0)$ in the N_1 - N_4 model (on $L = 1024$ lattices). The fugacities $w_4 = e^{-4}$ and e^{-3} correspond to concentrations $p_4 \approx 0.024$ and 0.065 , respectively. The solid line shows the asymptotic form r^{-2} .

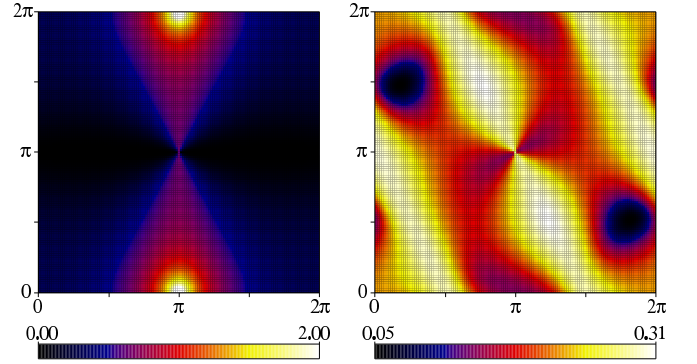


FIG. 5: Fourier transform of the dimer-dimer correlation D_1 of the N_1 model [left, for dimers pointing along $(1, 0)$] and D_4 of the N_4 model [right, for dimers pointing along $(2, 1)$] calculated on $L = 128$ lattices. In the left graph, the log-divergent peaks at $(\pi, 0)$ and $(\pi, 2\pi)$ have been cut-off at the value 2.0 (for this lattice size the peak value is ≈ 3.12)

size dependence up to the largest size ($L = 2048$) studied, although one might naively have expected a logarithmic divergence here as well, considering the r^{-2} real-space correlations.

Whereas the dimer correlations decay with a leading r^{-2} dependence, a drift in the exponent of the algebraic decay is manifest in the monomer correlations. Results for $M(r)$ at $r = L/2 - 1$ are shown multiplied by L^α in Fig. 6(a). Here α is adjusted to give a flat L dependence, and hence the critical form $M(r) \sim r^{-\alpha}$ is extracted. The known $\alpha = 1/2$ is used for the pure N_1 model. For the pure N_4 model the exponent is consistent with $\alpha = 1/9$ (to an accuracy of 1%). To show that the exponent changes from $1/2$ already at a low concentration of N_4 bonds, results for $w_4 = e^{-5}$ ($p_4 \approx 0.9\%$) are scaled with

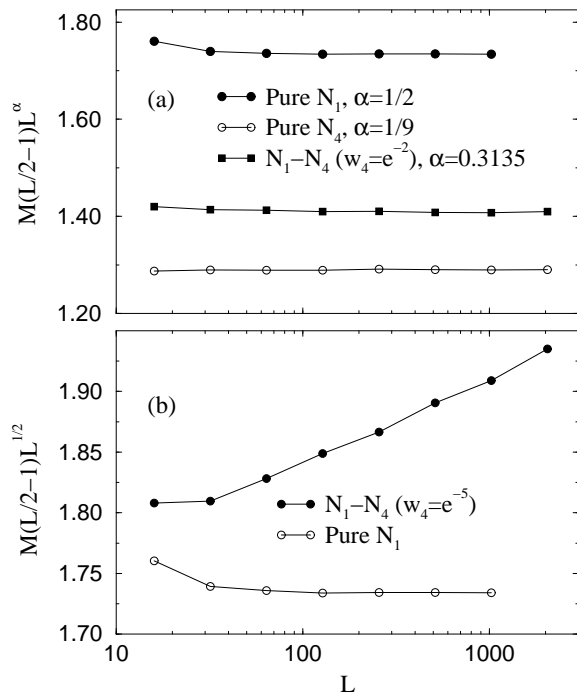


FIG. 6: Finite-size scaling of monomer correlations in the N_1 - N_4 model. (a) The best scaling for three different cases. (b) Failure of a scaling with the pure N_1 exponent $\alpha = 1/2$ for the N_1 - N_4 model at low fugacity w_4 .

$\alpha = 1/2$ in Fig. 6(b). This scaling clearly fails, and is instead consistent with $\alpha \approx 0.485$.

IV. ANALYTICAL RESULTS

We now present an analytical treatment of the numerical findings. We will in turn discuss exponents, correlation lengths, amplitudes and the angular form of the dimer correlations. Our discussion is based on the height model/Coulomb gas representation of bipartite dimer models on one hand,^{33,34,35} and on their large- N generalisation on the other.³⁶ The former is based on a mapping of the dimer configurations onto a fluctuating height surface and accounts for the gross features of the correlations described above. The latter reproduces in detail the features of the correlations of the N_4 model.

Let us start with a brief formulation of the height model for the bipartite N_1 - N_4 dimer model. This is analogous to Henley's work on the pure N_1 model.¹⁸ Readers interested in deeper detail are referred to Refs. 33,34,35.

Crucially, bipartiteness allows us to orient each dimer so as to point from one sublattice to the other. We can then assign to a dimer n units of a fictitious magnetic flux, \vec{B} , and to a link not occupied by a dimer m units of flux. The lattice divergence $\vec{\nabla} \cdot \vec{B} = 0$ if we choose $n + 11m = 0$, as in the N_1 - N_4 model, 11 of the 12 links emanate from a site are empty. It is convenient to choose the overall scale of \vec{B} so that $n = -11m = 11/12$. The

constraint $\vec{\nabla} \cdot \vec{B} = 0$ can be resolved in terms of a scalar height function, h , via $\vec{B} = \vec{\nabla} h$. (In $d = 2$, curl and grad are basically interchangeable). The crucial step in the height model ansatz is to posit that, upon coarse-graining, the entropy of the height surface gives rise to an energy functional containing a leading quadratic term of the form

$$E = \pi K \int d^2 \vec{r} |\vec{\nabla} h|^2. \quad (4)$$

Here, the (as yet undetermined) coupling constant K is known as the stiffness K .

Implicit in the derivation of such an energy functional of entropic origin is a coarse-graining procedure, which maps many microstates of the dimer model onto fewer macrostates.³⁵ In the process, other terms are generated both for the energy and in the identification of operators linking the height variable to, say, dimers and monomers. These terms are classified by an 'electromagnetic' charge, which, together with K , determines the exponent of the leading power of its correlations.^{33,34,35}

First, let us discuss the N_1 - N_2 model. N_2 dimers violate bipartiteness and thus show up as defects in the height surface; a finite density of such defects destroys the algebraic correlations. This was calculated analytically for a planar dimer model interpolating between the square and the triangular lattices by switching on only one of the two diagonal directions of next-nearest neighbour bonds. There, a dimer correlation length proportional to the inverse of the small fugacity was also found, which result was supplemented by an effective field theory arguing the same should hold true for monomer correlations in this system.²⁶ Our numerical results, in particular the scaling plots, confirm that these results hold also for the case of the nonplanar N_1 - N_2 model.

Next, we consider the N_1 - N_4 model. We first note that the monomer correlations have a power-law decay with an exponent given by K . The decrease of K from $1/2$ upon adding N_4 dimers, implies that the corresponding height model grows floppier (the heights fluctuate more strongly). We note in passing that it is rather straightforward to extract the monomer correlations using the directed-loop algorithm, as this only requires keeping track of the monomer separations in intermediate states sampled. This thus provides a means of determining the stiffness constant K with relatively little effort.

The analytical calculation of the dimer correlations are a little more involved than the monomers, as they contain two terms. One of them, the 'vertex term', decays with an exponent of $1/K$. The other, the 'dipolar term', always decays as $1/r^2$; which of these dominates depends on K , and for the pure N_1 model, they happen both to decay with the same power law. It is the vertex term which generates the logarithmic peak in the D_1 dimer structure factor in Fig. 5. Upon inclusion of N_4 dimers, i.e. with increasing K , the power of the decay becomes more rapid, and the divergence of this peak thus disappears when N_4 dimers are added.

The survival of the leading $1/r^2$ power in the dimer correlations is solely due to the dipolar term, which arises via the original identification of the dimers and $\vec{\nabla}h$ through the lattice flux \hat{B} : If we choose the vectors \hat{e}_k ($k = 1 \dots 12$) to point along the direction of a dimer from one sublattice to the other, we find a contribution to the dimer density n_k which is proportional to $\hat{e}_k \cdot \vec{B} = \hat{e}_k \cdot \vec{\nabla}h$. As long as the height correlations grow logarithmically with distance, $\langle (h(r) - h(0))^2 \rangle \propto \ln r$, as they do for the parameters our simulations probe, the resulting contribution to the dimer correlations always decay as $1/r^2$, on account of the derivative linking h and \vec{B} . As the power $1/K$ of the vertex term is only slightly larger than 2 for small values of w_4 , this leads to the very slow approach to the asymptotic $1/r^2$ behaviour, as evidenced in our simulations.

Despite their $1/r^2$ behaviour, the dipolar correlations do not yield a logarithmic peak in the structure factor. This is because their dipolar structure makes the leading term vanish as the angular part of the Fourier integral $\tilde{D}_A(\vec{q}) = \int dr d\phi \exp(i\vec{q} \cdot \vec{r}) D_A(r, \phi)$ is performed. Instead, what one finds are the characteristic bow-tie structures^{36,37,38} displayed in Fig. 5. These bow-ties are points of non-analyticity; there is no divergence, but a discontinuity there. The bow-ties reflect the transverse correlations of a divergence-free field \vec{B} . These bow-ties are thus oriented with one axis along the dimer under consideration.

It has recently been observed³⁶ that a semi-quantitative theory for such correlations can be obtained in the framework of a large- N generalisation of the hardcore dimer model, via an intermediate mapping to an Ising model, the ground-states of which are in correspondence with the dimer states. This Ising model is then solved in a self-consistent mean-field theory in the limit of low temperatures. We note that such a generalisation does not preserve the charge-assignments for the operators generated upon coarse-graining, and does therefore miss the vertex term and hence the logarithmic peak for the N_1 model. However, it does provide the angular dependence of the dipolar part of the correlations.

Here, we present the relevant theory for the dimer correlations both in the pure N_1 and the pure N_4 models. The former is of course also soluble in closed form. In either case, one assigns an Ising spin S to each *bond* of the lattice which encodes the presence ($S = +1$) or absence ($S = -1$) of a dimer on this bond.³⁶ The hardcore corresponds to a non-zero magnetisation in the model, but this leaves the shape of its $q \neq 0$ correlations unchanged.^{36,37}

In the case of the N_1 model, there are two bonds per unit cell (the links of the square lattice in the x and y directions), denoted by vectors \vec{v}_a , $\vec{v}_{1,2} = \hat{x}, \hat{y}$. The relevant interaction matrix, J , is thence a 2×2 matrix. Its Fourier transform is given by $\tilde{J}_{ab} = \cos(q_a/2) \cos(q_b/2)$. Here, $q_a = \vec{q} \cdot \vec{v}_a$, so that³⁹

$$\tilde{D}_A(\vec{q}) \sim \frac{\cos^2(q_y/2)}{\cos^2(q_x/2) + \cos^2(q_y/2)}. \quad (5)$$

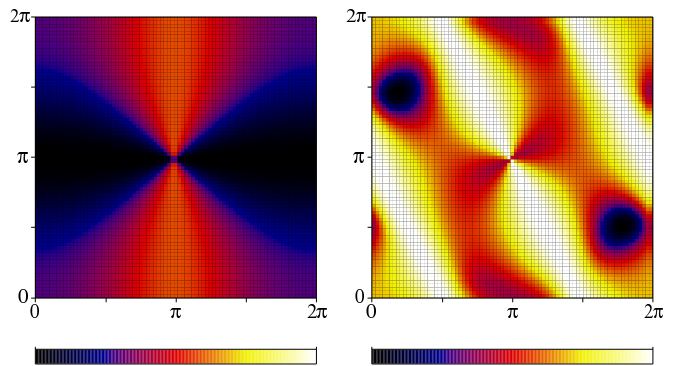


FIG. 7: Fourier transform of the dipolar part (i.e., without the dominant logarithmic peaks in N_1) of the dimer correlations D_1 of the N_1 model (left) and D_4 of the N_4 model (right), calculated from a large- N theory. The over-all amplitudes are not given accurately by the theory and are therefore not indicated here.

For the N_4 model, due to the non-planarity of the lattice on which the dimer model is defined, this theory takes a somewhat more complicated form. One now obtains a 4×4 interaction matrix. Again, let \vec{v}_a denote the four different dimer directions: $\vec{v}_{1,2} = (2, \pm 1)$, $\vec{v}_{3,4} = (\pm 1, 2)$. The same form of the interaction matrix as above then holds: $\tilde{J}_{ab} = \cos(q_a/2) \cos(q_b/2)$. We thus find the following correlations:

$$\tilde{D}_4(\vec{q}) \sim 1 - \frac{\cos^2(\vec{q} \cdot \vec{v}_1/2)}{\sum_{a=1}^4 \cos^2(\vec{q} \cdot \vec{v}_a/2)}. \quad (6)$$

These low-temperature spin (and hence approximate dimer) correlations are plotted in Fig. 7 above. We note that not only are the bow-ties of the simulation data, Fig. 5, reproduced in their correct orientation, but the qualitative structure of \tilde{D}_4 in reciprocal space is reproduced throughout.

V. CONCLUSIONS

The results obtained here demonstrate that the 2D square-lattice dimer model becomes deconfined when any finite density of non-bipartite (next-nearest-neighbor) dimers are introduced. The system remains algebraically confined in the presence of longer bipartite (fourth-nearest-neighbor) dimers, but the corresponding monomer exponent drifts. In contrast, as the stiffness of the corresponding height surface decreases, the leading dimer-dimer correlation exponent remains unchanged at $1/r^2$, due to the persistence of the dipolar term due to the gauge structure captured by the height model. Our results thus fit in with the known beliefs on dimer models and can be seen as a detailed check of their validity. We have shown that the directed-loop simulation algorithm can produce very accurate results for the drifting monomer exponent. In particular, the accuracy is high

enough to suggest the conjecture that this exponent for the pure N_4 model takes the rational value of $1/9$.

Our findings are relevant to quantum dimer models as well. Various resonance terms can be introduced, and corresponding RK points can then be demonstrated in the same way as has been done for other models.^{6,14,40} Hence, it is clear that an RVB state can in principle be realized on the square lattice once next-nearest-neighbor dimers are allowed. In the context of the dimer models for the Mott insulators relevant to the high- T_c cuprates, two points however need to be borne in mind. Firstly, the Rokhsar-Kivelson quantum dimer models allows a simple classical calculation at the RK point only if it is possible to choose the sign of the off-diagonal matrix elements to be negative, which property needs to be established on a case-by-case basis for non-bipartite models (it does hold for the bipartite case).⁴¹ In addition, the description of the singlet space using a dimer basis becomes overcomplete as the coordination of the dimer lattice increases. At any rate, our results again underscore the special im-

portance played by non-bipartiteness in the realisation of RVB liquids in $d = 2 + 1$.

Acknowledgments

We thank E. Fradkin, C. Henley, and S. Sachdev for discussions and comments on the manuscript. RM is grateful to P. Fendley, S. Isakov, W. Krauth, K. Gregor, K. Raman and S. L. Sondhi for collaboration on related work. In the initial stages of this work AWS was supported by the Academy of Finland, Project No. 26175. RM is supported in part by the Ministère de la Recherche et des Nouvelles Technologies with an ACI grant. This research was supported in part by the National Science Foundation under Grant No. PHY99-07949 at the KITP in Santa Barbara. Some of the simulations were carried out on the Condor system at the University of Wisconsin-Madison.

-
- ¹ R. H. Fowler and G. S. Rushbrooke, Trans. Faraday Soc. **33**, 1272 (1937).
 - ² M. E. Fisher, Phys. Rev. **124**, 1664 (1961).
 - ³ P. W. Kastelyn, Physica **27**, 1209 (1961); J. Math. Phys. **4**, 287 (1963).
 - ⁴ M. E. Fisher and J. Stephenson, Phys. Rev. **132**, 1411 (1963).
 - ⁵ S. A. Kivelson, D. S. Rokhsar, and J. P. Sethna, Phys. Rev. B **35**, 8865 (1987).
 - ⁶ D. S. Rokhsar and S. A. Kivelson, Phys. Rev. Lett. **61**, 2376 (1988).
 - ⁷ E. Fradkin, *Field theories of condensed matter systems* (Addison-Wesley, Redwood City 1991).
 - ⁸ T. Senthil and M. P. A. Fisher, Phys. Rev. B **62**, 7850 (2000).
 - ⁹ R. Moessner and S. L. Sondhi, Phys. Rev. Lett. **86**, 1881 (2001).
 - ¹⁰ C. Zeng and V. Elser, Phys. Rev. B **51**, 8318 (1995).
 - ¹¹ F. Mila, Phys. Rev. Lett. **81**, 2356 (1998).
 - ¹² G. Misguich, D. Serban, and V. Pasquier, Phys. Rev. Lett. **89**, 137202 (2002).
 - ¹³ S. Sachdev, Rev. Mod. Phys. **75**, 913 (2003).
 - ¹⁴ E. Ardonne, P. Fendley, and E. Fradkin, Ann. Phys. **310**, 493 (2004).
 - ¹⁵ P. W. Anderson, Mater. Res. Bull. **8**, 153 (1973); P. Fezekas and P. W. Anderson, Philos. Mag. **30**, 23 (1974).
 - ¹⁶ P. W. Anderson, Science **235**, 1196 (1987).
 - ¹⁷ This equivalence does not extend to monomer correlations: monomers at the RK point are deconfined whereas the classical models have confined monomers. In fact, the RK point is ‘deconfined multicritical’, sandwiched between two confining crystalline phases.^{9,23,24}
 - ¹⁸ C. L. Henley, J. Stat. Phys. **89**, 483 (1997).
 - ¹⁹ O. F. Syljuåsen, Int. J. Mod. Phys. B **19**, 1973 (2005).
 - ²⁰ C. Castelnovo, C. Chamon, C. Mudry, and P. Pujol, cond-mat/0502068.
 - ²¹ S. Sachdev, Phys. Rev. B **40**, 5204 (1989).
 - ²² P. W. Leung, K. C. Chiu, and K. J. Runge, Phys. Rev. B **54**, 12938 (1996).
 - ²³ E. Fradkin, D. A. Huse, R. Moessner, V. Oganesyan, and S. L. Sondhi, Phys. Rev. B **69**, 224415 (2004).
 - ²⁴ A. Vishwanath, L. Balents, T. Senthil, Phys. Rev. B **69**, 224416 (2004).
 - ²⁵ For a deformation of the square lattice hardcore dimer model using interactions between dimers, see F. Alet, J. L. Jacobsen, G. Misguich, V. Pasquier, F. Mila and M. Troyer, cond-mat/0501241.
 - ²⁶ P. Fendley, R. Moessner, and S. L. Sondhi, Phys. Rev. B **66**, 214513 (2002).
 - ²⁷ W. Krauth and R. Moessner, Phys. Rev. B **67**, 064503 (2003).
 - ²⁸ S. Sachdev and M. Vojta, J. Phys. Soc. Jpn **69**, Supp. B, 1 (2000).
 - ²⁹ O. F. Syljuåsen and A. W. Sandvik, Phys. Rev. E **66**, 046701 (2002).
 - ³⁰ The present method was first presented in an unpublished note: A. W. Sandvik, cond-mat/0312097.
 - ³¹ D. H. Adams and S. Chandrasekharan, Nucl. Phys. B **662**, 220 (2003).
 - ³² There is a rigorous result that any finite density of monomers destroys the critical correlations: O. J. Heilmann and E. H. Lieb, Phys. Rev. **24**, 1412 (1970).
 - ³³ B. Nienhuis, “Coulomb gas formulation of two-dimensional phase transitions,” in Phase Transitions and Critical Phenomena (C. Domb and J. Lebowitz, eds.) Academic Press, 1987.
 - ³⁴ For a recent detailed treatment of such theories, cf. J. L. Jacobsen and J. Kondev, Nucl. Phys. B **532**, 635 (1998).
 - ³⁵ For an introduction to height models close to the current perspective, cf. C. Zeng and C. L. Henley, Phys. Rev. B **55**, 14935 (1997).
 - ³⁶ S. V. Isakov, K. Gregor, R. Moessner and S. L. Sondhi, Phys. Rev. Lett. **93**, 167204 (2004); S. V. Isakov *et al.*, in preparation.

- ³⁷ C. L. Henley, Phys. Rev. B **71**, 014424 (2005)
- ³⁸ M. Hermele, M. P. A. Fischer and L. Balents, Phys. Rev. B **69**, 064404 (2004)
- ³⁹ By virtue of the equivalence of the square ice model and the ground states of the Ising model on the square lattice with crossings ('planar pyrochlore'), the large- N expression interaction matrix is also that studied in the latter context in B. Canals and D. Garanin, Eur. Phys. J. B **26**, 439 (2002)
- ⁴⁰ C. L. Henley, cond-mat/0311345.
- ⁴¹ K. S. Raman, R. Moessner and S. L. Sondhi, cond-mat/0502146.